Stacked U-Nets with Multi-Output for Road Extraction

Tao Sun, Zehui Chen, Wenxiang Yang, Yin Wang
Tongji University, Shanghai, China
{suntao, 1652763, twofyw, yinw}@tongji.edu.cn

Abstract

With the recent advances of Convolutional Neural Networks (CNN) in computer vision, there have been rapid progresses in extracting roads and other features from satellite imagery for mapping and other purposes. In this paper, we propose a new method for road extraction using stacked U-Nets with multiple output. A hybrid loss function is used to address the problem of unbalanced classes of training data. Post-processing methods, including road map vectorization and shortest path search with hierarchical thresholds, help improve recall. The overall improvement of mean IoU compared to the vanilla VGG network is more than 20%.

1. Introduction

Recent progresses in CNNs demonstrate significant improvements in typical computer vision tasks such as classification, object detection, localization, and semantic segmentation [1, 2, 3, 4, 5, 6]. Many application areas have been rapidly adapting these deep neural networks for better accuracy and efficiency With high-resolution satellite imagery, CNNs can extract roads and buildings that greatly assist the manual mapping process [7, 8, 9, 10, 11]. Because CNN models process one image patch of limited resolution at a time, there are two typical methods. One is the classification approach that predict the pixel labels of the center region of an image patch [7], using for example VGG nets [5], the other is the segmentation approach that labels all pixels of the entire image patch at once, including Full Convolutional Network (FCN) [12] and U-Net [13].

However, the process still requires significant human involvement due to limited prediction accuracy from the following reasons. First, roads and buildings are man-made objects that are very different from natural objects commonly seen in training datasets of computer vision research. Second, the mapping application has very low tolerance for small prediction errors such as road gaps due to vegetation or building shadow, and spurious roads due to parking lots or other pavements. Third, common knowledges and mapping conventions can be difficult for CNNs to learn. Last, image patch based models cannot capture macro features, e.g., road networks should be connected graphs, roads tend to follow shortest paths.

In this paper, we show that U-Nets have better mean IoU (mIoU) than VGG nets, and then propose a new model with stacked U-Nets that further improves mIoU. In addition, we use multiple output commonly seen in object localization. Post processing helps improve recall by connecting broken roads. Finally, a hybrid loss function can address the imbalanced training data problem.

2. Our Model

Figure 1 shows our CNN network based on the U-Net architecture [13]. In a nutshell, we concatenate two U-Nets to allow multiple output. The first U-Net outputs auxiliary information such as road topology and pixel distance to roads. The second U-Net generates road masks by classifying each pixel as road or non-road. We also extend the depth of the first U-Net from three to five to improve accuracy.

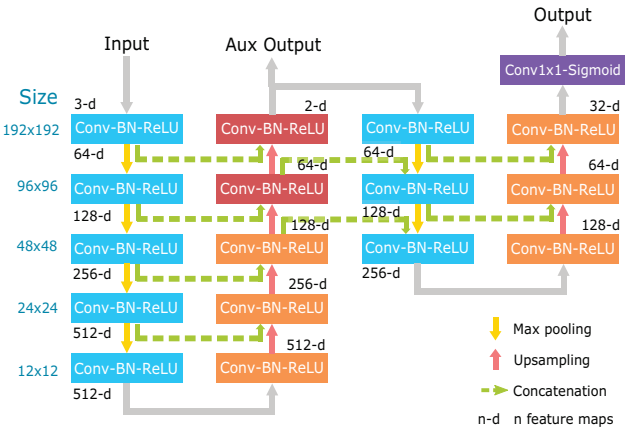

Figure 1. Stacked U-Net Overview

2.1. Stacking Units

A stacking unit is the basic component of our network. This unit consists of encoding blocks (marked cyan-blue) and decoding blocks (marked orange), shown in Figure 3.

2160-7516/18 $31.00 © 2018 IEEE
DOI 10.1109/CVPRW.2018.00033

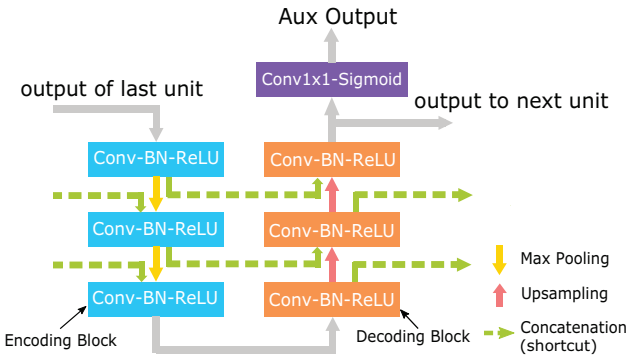

Figure 2. A stacking unit (three layers)

Encoding blocks and decoding blocks have linked shortcuts at the corresponding layers. These shortcuts ensure that the decoding blocks can utilize information from previous layers. The U-Net structure helps to combine feature maps from intermediate and deeper layers. Deeper layers usually contain high-level features, and swallow layers carry more details and location information. The shortcuts between different stacking units have similar effects. These shortcuts also benefit training convergence because gradients can propagate directly to early layers.

2.2. Encoding and Decoding Blocks

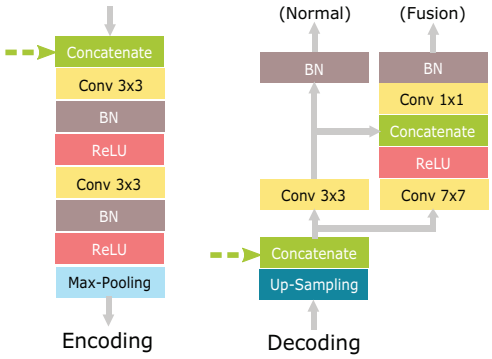

Figure 3. Encoding and decoding blocks

Similar to GoogleNet and Inception net, we use a branch-fusion block that concatenate feature maps from different size filters instead of a single 3x3 conv layer. This allows the network to recognize features of different sizes, and to learn how to merge the outputs in different channels.

3. Implementation

This section describes various optimization techniques in our implementation that boost the mean IoU.

3.1. Multiple Output

As described in Section 1, the CNNs often learn road appearance features such as colors, texture, and edges instead of structural features such as connectivity and consistent width of the same road.

Therefore, inspired by object localization and human post estimation CNN models, we add the following output to our network to force it to learn structural features, in addition to road pixel classfication output.

- the outgoing degree of a road pixel
- the distance of a pixel to the nearest roads

The degrees of different road pixels, which are calculated from ground truth automatically, help improve road connectivity by forcing the network to count outgoing branches. The pixel distance to the nearest road is calculated by *distance transformation*, which helps improve pixel classification accuracy where the road boundaries are ambiguous, e.g., dirt roads blending into field and roads half covered by vegetation [14]. This is similar to soft label frequently used in classification tasks. Figure 4 illustrates these additional outputs.

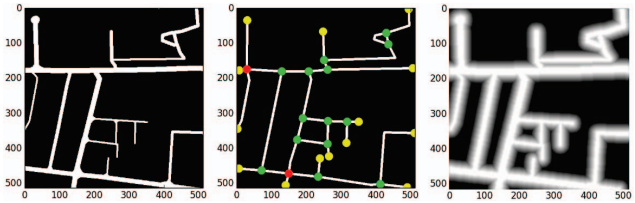

Figure 4. From left to right, ground truth, degree of a road pixel (yellow:1, white:2, green:3, red:4), and distance to nearest road shown in greyscale.

3.2. Post processing

Various post-processing techniques for road extraction have been proposed in the literature, e.g., centerline extraction using structured SVM [15] or Markov random field [9], handling noisy data using a special CNN [8], recovering lines by sampling junction-points [16], and bridging road gaps by heuristic search [11]. Here we develope a novel post processing technique by linking broken roads through shortest path search with decreasing confidence thresholds. More specifically, we first convert the raster road prediction image to vector format so we can bridge gaps and trim spurious roads, then we render a raster image from road vectors and merge it with the original prediction because the challenge needs raster images for IoU calculation.

3.2.1 Extracting Road Center Lines

We apply the same approach in [**?**] to extract road centerlines from the greyscale prediction image. First we apply a threshold to convert the greyscale image to black and white. Next, we evenly sample the contour line and draw the voronoi diagram. Only line segments completely covered by the threshold image is retained, which form the

road centerlines. We employ several optimization tweaks for cleaner road networks, including trimming road stubs and merging close intersections; see Fig. 5.

When rendering a raster image from road vectors, we need to know the road width, calculated from the average width along the road centerline using a dropoff threshold of 75% gray from the center.

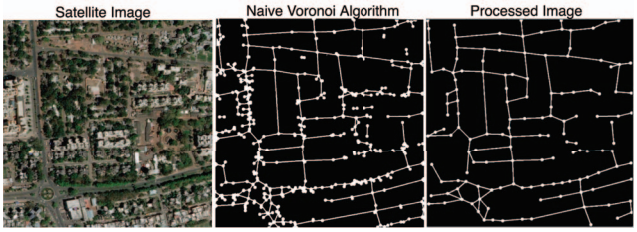

Figure 5. Centerline extraction using voronoi diagram

3.2.2 Connecting Broken Roads

Connecting broken roads helps improve recall significantly. Starting from a deadend in the vector road network extracted, we search possible connections to another existing road using the shortest path algorithm. We assign the cost of each pixel i as $c_i = -log[(p_i + \varepsilon)/(1 + \varepsilon)]$, where p_i is the road classification probability of the pixel. This forces the shortest path to prefer pixels with high probabilities of being roads, although not exceeding the threshold set in centerline extraction step above. It also prefers road centerlines instead of shortcuts along curved roads because centerlines typically have higher prediction probabilities. To further improve accuracy and speed, we apply shortest path search in multiple iterations with decreasing thresholds. We also set a maximum cost in each iteration so we only search a certain range for connection; see Algorithm 1. Here $U(s, \delta)$ denotes the neighborhood of s with radius δ. The list of decreasing threshold t_k we use is $\{0.5, 0.2, 0.1, 0.05, 0.01\}$ and δ is 100 pixels.

Fig.6 shows an example of the procedure. Areas in different colors represent the search ranges under different thresholds. Each iteration decreases the threshold and therefore increases the search range. The iterative search result in (F) is bbetter than a one-pass search in (B). It is also faster because each iteration only searches a small range of pixels.

3.3. Hybrid loss function

The cross-entropy loss with our unbalanced training data leads to slow convergence and low accuracy. We add the Jaccard loss into our loss function $L = L_{ce} - \lambda \log L_{jaccard}$, where

$$L_{ce} = -\frac{1}{N}\sum_{i=0}^{N}(y \log y' + (1-y)\log(1-y')) \quad (1)$$

$$L_{jaccard} = \frac{1}{N}\sum_{i=0}^{N}\frac{y_i y_i'}{y_i + y_i' - y_i y_i'} \quad (2)$$

Algorithm 1 Threshold decreasing

Require: The topological graph of road map, $T_{n,m}$; The predicted labels map, $P_{n,m}$; The thresholds list, t_k;
Ensure: The gap-connected road map Q;

```
Q ← T;
for each t in t_k do
    for all 1-degree point s with another 1-degree point exists in Ů(s, δ) do
        P' ← threshold by range [t_k, t_{k-1}]
        ΔQ ← PathSearch(P', s, t);
        Q ← Q ∪ ΔQ;
    end for
end for
return Q;
```

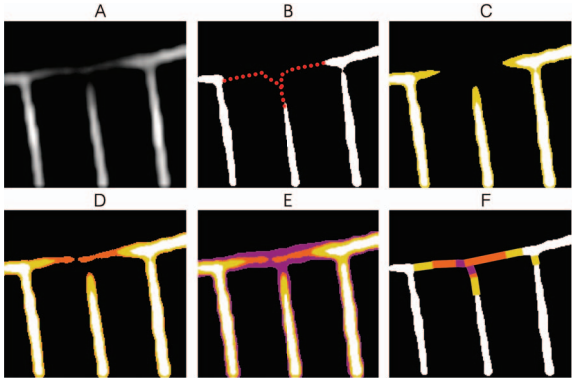

Figure 6. Connecting broken roads. A: original prediction; B: one-pass search, C - E: different iterations with decreasing threshold; F: final results.

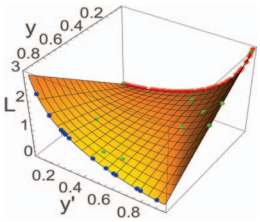

Figure 7. Cross Entropy Surface

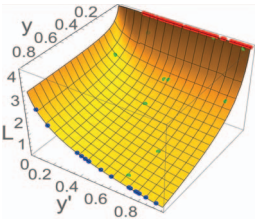

Figure 8. Jaccard Surface

Here y and y' mean the target and prediction vectors, respectively, and λ is the weight of the Jaccard loss[18]. For cross entropy loss, the imbalance of sample points (97%neg. vs 3%pos.) makes direction of gradient decreasing toward the back conner (Fig.7), which leads to a local optimum, especially in the early stage. The Jaccard loss effectively "lifts up" the back conner, and helps to avoid the local optimum; see Fig. 8.

4. Experiments

Our experiments are performed on DeepGlobe dataset [19]. Our network is trained using Keras with the Tensor-

Figure 9. Illustration of prediction and post-processing. The three figures in a row are the satellite image, the prediction output with post-processing add-on in red, and the ground truth.

Flow backend. Data augmentation, including rotation, flipping, and cropping, help avoid over fitting. We pretrained the first U-Net, and fine tune the whole nets using different settings. Adam optimizer with the initial learning rate of 0.001 works for us. We further reduce learning rate by 10x if the loss stop decreasing during the last 10 epochs.

Multi-output improves our U-Net about 2% in mIoU (Fig.10). Different λ values in the loss function have significant impact in the accuracy. The proper $\lambda = 30$ boosts the performance most (Tab.1). In addition, if the "cross entropy" is not included, then the network cannot converge, because gradient disappears for all negative samples. Patch overlapping also contributes to the accuracy. Tab.2 shows the overall scores of different settings.

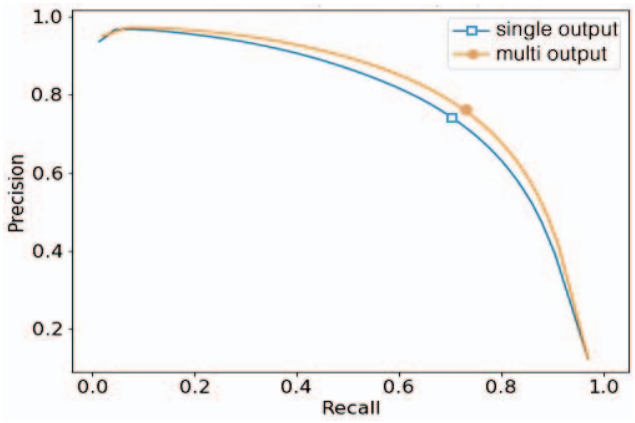

Figure 10. PR curve of single output and multi outputs (Our Unet with Overlap 16x)

5. Conclusion

We developed a stacked U-Nets for road extraction using satellite imagery. Various optimization techniques such as multiple outputs, post processing of shortest path searching with decreasing thresholds, and hybrid loss are used to achieve more than 20% mIoU increase over the plain VGG net. After our optimization, currently the most significant problem is the poor prediction in rural areas, where the roads are very obscure and the ground truth could be ambiguous.

Table 1. Impact of hybrid loss function (on validation set)

λ	mIoU (%)	Precision (%)	Recall (%)
1	42.2	70.8	59.2
10	45.3	65.0	60.9
20	47.1	**71.6**	61.6
30	**49.0**	68.3	64.7
40	48.3	66.0	**65.7**

Table 2. Performance of different networks

Networks	mIoU (%)
VGG-19 (w/o multi output)	38.4
VGG-19 (with multi output)	39.3
U-Net (w/o multi output)	42.9
U-Net (with multi output)	44.3
Our U-Net (w/o multi output)	45.6
Our U-Net (with multi output)	**47.1**
Our U-Net (multi + overlap 8x)	53.6
Our U-Net (multi + overlap 16x)	56.8
Our U-Net (multi + overlap 16x + post)	**60.0**

References

[1] Volodymyr Mnih and Geoffrey E. Hinton. Learning to detect roads in high-resolution aerial images. In Kostas Daniilidis, Petros Maragos, and Nikos Paragios, editors, *Computer Vision – ECCV 2010*, pages 210–223, Berlin, Heidelberg, 2010. Springer Berlin Heidelberg.

[2] Alex Krizhevsky, Ilya Sutskever, and Geoffrey E Hinton. ImageNet Classification with Deep Convolutional Neural Networks. *NIPS*, 2012.

[3] Pierre Sermanet, David Eigen, Xiang Zhang, Michael Mathieu, Rob Fergus, and Yann LeCun. OverFeat: Integrated Recognition, Localization and Detection using Convolutional Networks. *arXiv.org*, December 2013.

[4] Matthew D Zeiler and Rob Fergus. Visualizing and Understanding Convolutional Networks. In *ECCV*. Springer, Cham, Cham, September 2014.

[5] Karen Simonyan and Andrew Zisserman. Very Deep Convolutional Networks for Large-Scale Image Recognition. *CoRR*, 2014.

[6] Kaiming He, Xiangyu Zhang, Shaoqing Ren, and Jian Sun. Deep Residual Learning for Image Recognition. In *CVPR*, 2016.

[7] Volodymyr Mnih and Geoffrey E. Hinton. Learning to detect roads in high-resolution aerial images. In *Computer Vision - ECCV 2010 - European Conference on Computer Vision, Heraklion, Crete, Greece, September 5-11, 2010, Proceedings*, pages 210–223, 2010.

[8] Volodymyr Mnih and Geoffrey E Hinton. Learning to Label Aerial Images from Noisy Data. *ICML*, 2012.

[9] Gellért Máttyus, Shenlong Wang, Sanja Fidler, and Raquel Urtasun. Enhancing Road Maps by Parsing Aerial Images Around the World. *ICCV*, pages 1689–1697, 2015.

[10] Yin Wang. Scaling Maps at Facebook. In *SIGSPATIAL*, 2016. keynote.

[11] Gellért Máttyus, Wenjie Luo, and Raquel Urtasun. DeepRoadMapper - Extracting Road Topology from Aerial Images. *ICCV*, pages 3458–3466, 2017.

[12] E. Shelhamer, J. Long, and T. Darrell. Fully convolutional networks for semantic segmentation. *IEEE Trans. on PAMI*, 39(4):640–651, April 2017.

[13] Olaf Ronneberger, Philipp Fischer, and Thomas Brox. U-Net: Convolutional Networks for Biomedical Image Segmentation. In *Medical Image Computing and Computer-Assisted Intervention – MICCAI 2015*, pages 234–241. Springer International Publishing, Cham, November 2015.

[14] Benjamin Bischke, Patrick Helber, Joachim Folz, Damian Borth, and Andreas Dengel. Multi-Task Learning for Segmentation of Building Footprints with Deep Neural Networks. *CoRR*, 2017.

[15] Elisa Ricci and Renzo Perfetti. Large Margin Methods for Structured Output Prediction.

[16] Dengfeng Chai, Wolfgang Förstner, and Florent Lafarge. Recovering Line-Networks in Images by Junction-Point Processes. *CVPR*, 2013.

[17] Xuemei Liu, James Biagioni, Jakob Eriksson, Yin Wang, George Forman, and Yanmin Zhu. Mining large-scale, sparse gps traces for map inference: Comparison of approaches. In *Proceedings of the 18th ACM SIGKDD International Conference on Knowledge Discovery and Data Mining*, KDD '12, pages 669–677, New York, NY, USA, 2012. ACM.

[18] Maxim Berman, Amal Rannen Triki, and Matthew B Blaschko. The Lovász-Softmax loss: A tractable surrogate for the optimization of the intersection-over-union measure in neural networks. *arXiv.org*, May 2017.

[19] David Lindenbaum Guan Pang Jing Huang Saikat Basu Forest Hughes Devis Tuia Ramesh Raskar Ilke Demir, Krzysztof Koperski. DeepGlobe 2018: A Challenge to Parse the Earth through Satellite Images. *arXiv.org*, 2018.